Attractive and repulsive Casimir vacuum energy with general boundary conditions

M. Asorey [a,*], J.M. Muñoz-Castañeda [b]

[a] *Departamento de Física Teórica, Facultad de Ciencias, Universidad de Zaragoza, E-50009 Zaragoza, Spain*
[b] *Institut für Theoretische Physik, Universität Leipzig, Brüderstr. 16, D-04103 Leipzig, Germany*

Abstract

The infrared behaviour of quantum field theories confined in bounded domains is strongly dependent on the shape and structure of space boundaries. The most significant physical effect arises in the behaviour of the vacuum energy. The Casimir energy can be attractive or repulsive depending on the nature of the boundary. We calculate the vacuum energy for a massless scalar field confined between two homogeneous parallel plates with the most general type of boundary conditions depending on four parameters. The analysis provides a powerful method to identify which boundary conditions generate attractive or repulsive Casimir forces between the plates. In the interface between both regimes we find a very interesting family of boundary conditions which do not induce any type of Casimir force. We also show that the attractive regime holds far beyond identical boundary conditions for the two plates required by the Kenneth–Klich theorem and that the strongest attractive Casimir force appears for periodic boundary conditions whereas the strongest repulsive Casimir force corresponds to anti-periodic boundary conditions. Most of the analysed boundary conditions are new and some of them can be physically implemented with metamaterials.
© 2013 Elsevier B.V. All rights reserved.

Keywords: Vacuum energy; Casimir effect; Boundary conditions

1. Introduction

The role of boundaries in quantum field theory has been a focus of increasing activity in different areas of physics. In general, the presence of boundaries enhances quantum aspects of

---

* Corresponding author.
  E-mail addresses: asorey@unizar.es (M. Asorey), jose.munoz-castaneda@uni-leipzig.de (J.M. Muñoz-Castañeda).

the system. Boundary properties have been known to play an important role in Casimir effect [1] since the early days of quantum field theory. More recently it has become a basic ingredient in the analysis of the very first principles of fundamental physics: black hole quantum physics quantum holography, string theories and D-branes and AdS/CFT dualities.

Boundary phenomena determine the structure of the quantum vacuum and the low energy behaviour of the quantum field theories. In massless theories these effects are amplified because the existence of long distance correlations allow boundary effects to percolate throughout the whole bulk region. In that case the vacuum energy is highly dependent on the geometry of the physical space and the physical properties of the boundaries encoded by boundary conditions [2–13].

In this paper we focus on the dependence of vacuum energy on boundary conditions in a massless field theory confined to a domain bounded by two homogeneous parallel plates. The dependence of this energy with the distance between the plates is the basis of Casimir effect. Indeed, the variation of vacuum energy due to vacuum fluctuations induces a force between the plates. If the plates are identical this force is attractive as demonstrates the Kenneth–Klich theorem [14]. In general, this theorem shows that due to the general principles of quantum field theory the force induced by quantum vacuum fluctuations between two identical but not necessary planar bodies is always attractive. However, it is of enormous interest to get physical configurations where the Casimir force is repulsive instead of attractive, not only by its relevance for technical applications to micro-mechanical devices (MEMS), but also because the existence of repulsive or null Casimir forces allows a more accurate analysis of micro-gravity effects. There are recent conjectures about the violation of Newton gravitational law at sub-millimeter scales (see Refs. [15–17]) and to clarify the possible physical deviations at this short distances regime it is essential to disentangle gravitational effects from Casimir force (see Refs. [18–20]). In this study the control of Casimir forces is essential and in repulsive Casimir regimes is easier to discriminate from gravitational effects.

All methods used to achieve a repulsive Casimir effect are based on plates with different properties. In fact, new repulsive regimes of the Casimir effect have been found between different dielectric plates [21], and between a metallic plate with a hole and a needle pointing to the hole center [22]. In this paper we consider the most general boundary conditions for two plates which turn out to depend on four parameters to analyse in great detail the transition from attractive to repulsive Casimir regimes [23–27], with particular emphasis on the characterisation of Casimir-less boundary conditions in the interface of both regimes [26]. Although in practice, only some of these boundary conditions can be physically implemented, the advances in nano-science allow to the construction of new materials (metamaterials) with very special characteristics, which may allow, in the near future, the implementation of new types of boundary conditions.

2. Vacuum energy of bosonic massless fields in bounded domains

The infrared properties of quantum field theory are very sensitive to boundary conditions [28]. In particular the physical properties of the quantum vacuum state and the vacuum energy exhibit a very strong dependence on the type of boundary conditions.

One of the most important effects of boundaries in field theories is the appearance of Casimir effect. Within the global framework of boundary conditions formulated above we can analyse with complete generality which boundary conditions generate attractive or repulsive Casimir forces, i.e. the scope of attractive and repulsive regimes in the Casimir effect.

Let us consider, for simplicity, a free massless complex scalar field ψ confined in a domain $\Omega \subset \mathbb{R}^D$ bounded by two parallel homogeneous plates. Let us assume that the parallel plates are

orthogonal to the OX_D direction and are placed at $x_D = 0$ and $x_D = L$, respectively. Although physically interesting systems are three-dimensional ($D = 3$), for some interesting applications we also consider two-dimensional systems ($D = 2$). The results can be easily generalised for massless fermions and gauge theories.

The Hamiltonian is given by

$$\widehat{\mathbf{H}} = \frac{1}{2} \int_{\Omega} d^D \mathbf{x} \left(|\widehat{\pi}(\mathbf{x})|^2 - \widehat{\psi}^*(\mathbf{x}) \Delta \widehat{\psi}(\mathbf{x}) \right), \tag{2.1}$$

with standard canonical quantization commutation rules

$$\left[\widehat{\pi}(\mathbf{x}), \widehat{\psi}(\mathbf{x}') \right] = -i\hbar \delta(x - x'), \tag{2.2}$$

which describes an infinite number of decoupled harmonic oscillators given by the Fourier modes of the operator $-\Delta$. Unitarity requires that the Hamiltonian (2.1) has to be selfadjoint which is the case if all oscillating frequencies of these harmonic oscillators are real and non-negative. This requirement can be fulfilled if and only if all eigenvalues of the Laplacian operator $-\Delta$ are real and non-negative, i.e. $-\Delta$ is a non-negative selfadjoint operator.

Because of the homogeneity of the plates the boundary conditions must be invariant under translation along the plates. Local boundary conditions of physical states ψ in the domains of the selfadjoint extensions of $-\Delta$ have been characterised in Ref. [29] in terms of 2×2 unitary matrices $U \subset U(2)$. They are given by

$$\varphi - i\delta\dot{\varphi} = U(\varphi + i\delta\dot{\varphi}), \tag{2.3}$$

where

$$\varphi = \begin{pmatrix} \varphi(L) \\ \varphi(0) \end{pmatrix}, \qquad \dot{\varphi} = \begin{pmatrix} \dot{\varphi}(L) \\ \dot{\varphi}(0) \end{pmatrix}, \tag{2.4}$$

are the boundary values $\varphi = \psi|_{\partial\Omega}$ of the states ψ and their outward normal derivatives $\dot{\varphi} = \partial_n \psi|_{\partial\Omega}$ on the plates, and δ is an arbitrary characteristic length parameter.

However, non-negativity imposes a further constraint [24–26] on boundary conditions (2.3). Indeed, any state ψ whose boundary values φ are eigenvalues of the unitary operator $U\varphi = e^{i\alpha}\varphi$ verifies the identity [29]

$$\langle \psi, -\Delta_U \psi \rangle = \|d\psi\|^2 + \delta^{-1} \tan\frac{\alpha}{2} \|\varphi\|^2,$$

which implies that the selfadjoint extension $-\Delta_U$ can be non-negative for large enough volumes only if $\pi < \alpha < 2\pi$. For simplicity, from now we shall assume $\delta = 1$.

In the standard parametrisation of $U(2)$ matrices

$$U(\alpha, \beta, \mathbf{n}) = e^{i\alpha}(\mathbb{I}\cos\beta + i\mathbf{n} \cdot \boldsymbol{\sigma} \sin\beta), \quad \alpha \in [0, 2\pi], \ \beta \in [-\pi/2, \pi/2] \tag{2.5}$$

in terms of an unitary vector $\mathbf{n} \in S^2$ and Pauli matrices $\boldsymbol{\sigma}$, the space of boundary conditions $\mathcal{M}_F$ which give rise to positive selfadjoint extensions of $-\Delta$ is reduced to

$$\mathcal{M}_F \equiv \left\{ U(\alpha, \beta, \mathbf{n}) \in U(2) \mid 0 \leqslant \alpha \pm \beta \leqslant \pi \right\}, \tag{2.6}$$

since the eigenvalues of U are $e^{i(\alpha \pm \beta)}$.

The boundaries of the space $\mathcal{M}_F$ are the Cayley submanifolds $\mathcal{C}_{\pm}$ [29] given by unitary operators U having at least one real eigenvalue[1] $\lambda = \pm 1$ ($\alpha = 0, \pi$). The rich structure of this space includes very sophisticated boundary conditions which have never been considered in field theory in bounded domains. Most of the boundary conditions are non-local and some of them can be experimentally implemented coating the boundary with suitable metamaterials. Some of them involve topology changes [30,29] which motivated recent interesting proposals related to quantum gravity [31,32].

The vacuum state of the scalar free field theory with boundary condition $U \in \mathcal{M}_F$ is unique and given by

$$\Psi_0(\psi) = \mathcal{N} e^{-\frac{1}{2}(\psi, \sqrt{-\Delta_U}\psi)} \tag{2.7}$$

in the functional Schrödinger representation, $\mathcal{N}$ being a normalisation constant. The energy corresponding to the Gaussian vacuum state $\Psi_0(\psi)$ is given by the sum of the eigenvalues of $\sqrt{-\Delta_U}$, i.e.

$$E_U = \operatorname{tr} \sqrt{-\Delta_U}. \tag{2.8}$$

Notice the absence of the $\frac{1}{2}$ factor because of the complex nature of the fields. For scalar real fields the Casimir energy is $\frac{1}{2}$ of the result for complex scalars with the restriction that only boundary conditions with $U = U^{\top}$ (i.e. $n_2 = 0$ for parallel plates) should be considered [33]. In present case of conformal massless theories the infrared properties of the theory are enhanced and the genuine Casimir effect is stronger. In this regime the dependence on the boundary conditions of the fields also becomes more significant. In fact in the case of boundary conditions with zero-modes the vacuum state becomes unbounded and ill-defined. The problem disappears if the scalar field is compactified (see Refs. [34,35]). Although the contribution of the zero-modes to the boundary entropy at finite temperature is crucial [35] they do not contribute to the vacuum Casimir energy.

The sum $\operatorname{tr} \sqrt{-\Delta_U}$ is ultraviolet divergent but there are finite volume corrections to the vacuum energy density which give rise to a finite neat Casimir effect. The divergences can be regularised using the heat equation kernel method [36–38]. Indeed, we replace the divergent expression (2.8) by

$$E_U^{\epsilon} = \operatorname{tr} \sqrt{-\Delta_U} e^{-\epsilon \Delta_U}, \tag{2.9}$$

where ϵ is the ultraviolet regularisation parameter with units of inverse energy. The field theory is defined in the physical limit $\epsilon \to 0$. Before taking the physical limit we can make an asymptotic expansion in the distance L between plates to obtain the regularised expression of the vacuum energy between the plates, which behaves as

$$\frac{E_U^{(L,\epsilon)}}{S} = c_0 \epsilon^{-D/2 - 1/2} L + c_1 \epsilon^{-D/2} + \frac{c^{(D)}}{L^D} + \mathcal{O}\left(\frac{\epsilon^{\frac{1}{2}}}{L^{D+1}}\right), \tag{2.10}$$

where S is the (infinite) volume of the plates. In the regularised L expansion (2.10) each term has a different physical meaning:

---

[1] Cayley submanifolds $\mathcal{C}_{\pm}$ have a stratified structure characterised by the multiplicities of the eigenvalues ± 1.

1. The first term $c_0 \epsilon^{-D/2-1/2}$ is the energy density of the field theory in the bulk

$$c_0 = \frac{\epsilon^{D/2+1/2}}{(2\pi)^D} \int d^D k \, |k| e^{-\epsilon k^2} = \frac{\Gamma(\frac{D+1}{2})}{(4\pi)^{\frac{D}{2}} \Gamma(\frac{D}{2})} \tag{2.11}$$

   and does not depend on the boundary conditions but is ultraviolet divergent.

2. The second term $c_1 \epsilon^{-D/2}$ is the surface energy density associated to the plates. It presents a lower degree of ultraviolet divergence and depends on boundary conditions.

3. The third term constitutes the first finite contribution to the vacuum energy

$$E_U^{(L)} = \frac{c^{(D)}}{L^D} S, \tag{2.12}$$

   and defines the Casimir energy. The corresponding Casimir force

$$F_U^{(L)} = D \frac{c^{(D)}}{L^{D+1}} S \tag{2.13}$$

   is suppressed by the L^{-D-1} power law and its character can be attractive or repulsive, depending on the sign of the coefficient $c^{(D)}$.

To determine the attractive or repulsive nature of the Casimir force we calculate the coefficient $c^{(D)}$ as a function of the consistent boundary conditions given by unitary operators $U \in \mathcal{M}_F$.

The spectrum of Δ_U has a continuous component indexed by $D-1$ coordinates, whereas the compact and bounded direction orthogonal to the plates generate a discrete component in the spectrum, which will depend on the boundary condition defined by U, i.e.

$$\lambda_{i,\mathbf{k}} = \kappa_i^2 + \sum_{j=1}^{D-1} k_j^2,$$

where $\mathbf{k} = (k_1, \ldots, k_{D-1})$ is any vector of $\mathbb{R}^{D-1}$ and κ_i^2, $i = 0, 1, \ldots, \infty$, are the eigenvalues of the operator

$$-\Delta_U^{(D)} = -\frac{d^2}{dx_D^2}$$

acting on functions defined in $[0, L]$ with boundary conditions (2.3).

Therefore the functional trace can be written in the form

$$\text{tr}(-\Delta_U)^{1/2} e^{-\epsilon \Delta_U} = \frac{S}{(2\pi)^{D-1}} \sum_{i=0}^{\infty} \int d^{D-1}\mathbf{k} \, e^{-\epsilon(\mathbf{k}^2+\kappa_i^2)} \sqrt{\mathbf{k}^2 + \kappa_i^2},$$

where S is the infinite $(D-1)$-volume of the plates. Performing the change of variables $q_j = k_j/\kappa$ we obtain

$$\text{tr}(-\Delta_U)^{1/2} e^{-\epsilon \Delta_U} = \frac{S}{(2\pi)^{D-1}} \sum_{i=0}^{\infty} \kappa_i^D \int d^{D-1}\mathbf{q} \, e^{-\epsilon \kappa_i^2(\mathbf{q}^2+1)} \sqrt{\mathbf{q}^2 + 1},$$

and using generalised spherical coordinates, once the angular variables are integrated out, we obtain

$$E_U^{(D)}(\epsilon) = \frac{S\Omega_{D-2}}{(2\pi)^{D-1}} \sum_{i=0}^{\infty} \kappa_i^D \int_0^{\infty} dq \, e^{-\epsilon \kappa_i^2(q^2+1)} q^{D-2} \sqrt{q^2 + 1},$$

where

$$\Omega_{D-2} = 2\frac{\pi^{\frac{D-1}{2}}}{\Gamma(\frac{D-1}{2})}$$

is the area of the $(D-2)$-sphere. The q-integral can be expressed in terms of the confluent hypergeometric function $U(a, b, z)$ as

$$\int_0^\infty dq\, e^{-\epsilon\kappa^2(q^2+1)} q^{D-2} \sqrt{q^2+1} = \frac{1}{2}\Gamma\left(\frac{D-1}{2}\right) U\left(\frac{D-1}{2}, \frac{D}{2}+1, \epsilon\kappa^2\right) e^{-\epsilon\kappa^2},$$

(2.14)

for any values of $D > 0$ and $\epsilon > 0$. Therefore the regularised vacuum energy per unit volume of the plates can be written as

$$\frac{E_U^{(D)}(\epsilon)}{S} = \frac{1}{2^{D-1}\pi^{\frac{D-1}{2}}} \sum_{i=0}^\infty \kappa_i^D e^{-\epsilon\kappa_i^2} U\left(\frac{D-1}{2}, \frac{D}{2}+1, \epsilon\kappa_i^2\right).$$

(2.15)

To perform the sum we have to calculate the eigenvalues κ_i^2. They can be found by imposing the boundary conditions (2.3) on the wave functions of the domain of the selfadjoint extension $-\Delta_U^{(D)}$

$$\psi_k(x) = C_1 e^{-ikx} + C_2 e^{ikx},$$

(2.16)

which give rise to a linear homogeneous equation for the coefficients C_1 and C_2,

$$(M - UN)\begin{pmatrix} C_1 + C_2 \\ C_1 - C_2 \end{pmatrix} = 0$$

(2.17)

where M and N are the 2×2 complex matrices

$$M = \begin{pmatrix} 1 & -k \\ \cos kL + ik\sin kL & k\cos kL + i\sin kL \end{pmatrix},$$

(2.18)

$$N = \begin{pmatrix} 1 & k \\ \cos kL - ik\sin kL & -k\cos kL + i\sin kL \end{pmatrix}.$$

(2.19)

Matrices M and N are the linear maps from the scattering data into the boundary values. These maps will become infinite-dimensional in higher-dimensional spacetimes. The linear system (2.17) has non-trivial solutions if and only if $\det(M - UN) = 0$. Thus, the eigenvalues κ_i^2 of $-\Delta_U^{(D)}$ are given by the zeros of the spectral function (see Ref. [23])

$$\begin{aligned} h_U(k) &= \det(M - UN) \\ &= 4k\det U\cos kL - 2i(1+k^2)\det U\sin kL + 4k(U_{21} + U_{12}) \\ &\quad - 2i(1+k^2)\sin kL - 4k\cos kL + 2i(1-k^2)\operatorname{tr} U\sin kL. \end{aligned}$$

These zeros provide the eigenvalues of $-\Delta_U^{(D)}$ with one exception: the zero modes $k = 0$. In this case the maps M and N have to be modified because the plane wave parametrisation of scattering becomes degenerate and does not account for all possible zero-mode eigenfunctions. However

the information about the zero-modes of $-\Delta_U^{(D)}$ for any $U \in \mathcal{M}_F$ is encoded in $h_U(k)$ [39]. Using parametrisation (2.5) we can write the spectral function $h_U(k)$ as

$$h_U(k) = 2i e^{i\alpha}\big[\sin(kL)\big((k^2 - 1)\cos(\beta) + (k^2 + 1)\cos(\alpha)\big)$$
$$- 2k \sin(\alpha)\cos(kL) - 2kn_1 \sin(\beta)\big]. \tag{2.20}$$

The apparent lack of dimensional homogeneity of the k powers is due to the fact that we have chosen $\delta = 1$ in the boundary conditions (2.3). In general they should be considered as powers of the dimensionless variable $k\delta$.

The spectral function is not only dependent on the algebraic invariants of the boundary unitary matrix $\det U$ and $\operatorname{tr} U$ but also on the entries U_{21} and U_{12}, which implies that the spectrum of the quantum theory will be different for U matrices with the same eigenvalues even when they are equivalent as matrices. Of note is that all the zeros of the spectral function h_U lay on the positive real line of the complex k-plane because the consistency conditions ensure the non-negativity of the selfadjoint extension $-\Delta_U^{(D)}$ when $U \in \mathcal{M}_F$.

The sum over the eigenvalues of the operator $(-\Delta_U^{(D)})^{\frac{1}{2}}$ is equivalent to the sum over the zeros of the spectral function $h_U(k)$. Null eigenvalues which are incorrectly described by h_U do not contribute in both cases. Since $h_U(k)$ is holomorphic in k, using the argument principle, the summation over zeros can be rewritten in terms of an contour integral enclosing all the zeros of h_U (see Refs. [42–44,36,37] for more details). Indeed because of the consistency conditions all zeros of h_U are contained in $\mathbb{R}^+$ and by using Cauchy's residues theorem

$$\frac{E_U^{(D)}(\epsilon)}{S} = \sum_{n=0}^{\infty} k_n e^{-\epsilon\kappa_n^2} U\left(\frac{D-1}{2}, \frac{D}{2} + 1, \epsilon\kappa_i^2\right)$$
$$= \frac{1}{2\pi i} \oint dk\, k e^{-\epsilon k^2} U\left(\frac{D-1}{2}, \frac{D}{2} + 1, \epsilon k^2\right) \frac{d}{dk}\log\big(h_U(k)\big), \tag{2.21}$$

where the integration contour encloses a thin strip around all the positive real axis which includes all the zeros of h_U. The zeros of the spectral function generate simple or double poles (depending on eigenvalue degeneracies) of the logarithmic derivative $\frac{d}{dk}\log h_U(k)$. There are many similar integral formulas in the Casimir literature [45–48] (see [8] for more complete list of references, and [36] for a review of spectral techniques in quantum field theory), but most of them do not apply to the very general type of boundary conditions that we are considering.

In the limit $\epsilon \to 0$ the expression (2.21) diverges as indicated by the asymptotic expansion (2.10). To extract the finite part of this expression, that contains the Casimir energy, we have to subtract not only the leading divergence of the vacuum energy induced from fluctuations of the fields in the bulk but also remove the subleading divergent contribution associated with the self-energy of the boundaries. The later can be achieved by subtracting the vacuum energy of an identical system with the same boundary condition defined over a fixed reference size $L_0 < L$. After both subtractions a finite value for the Casimir energy is obtained

$$\frac{c_U^{(D)}}{L^D} = \frac{L_0^D}{L^D - L_0^D} \lim_{\epsilon\to 0}\left(c_0^{(D)}(\epsilon)(L - L_0) - \frac{1}{S}\big(E_U^{(L)}(\epsilon) - E_U^{(L_0)}(\epsilon)\big)\right). \tag{2.22}$$

Thus, the Casimir energy is given by the finite part of (2.21) which can be obtained by first removing the $\epsilon^{-\frac{D+1}{2}}$ and $\epsilon^{-\frac{D}{2}}$ divergent terms of $E_U^{(D)}(\epsilon)$ and then taking the physical limit $\epsilon \to 0$. The behaviour of the finite contribution of (2.21) is strongly dependent on the parity,

even or odd, of the spacial dimension D because of the different asymptotic behaviours of the confluent hypergeometric function $U(a, b, z)$.

In the odd case $D = 2n + 1$ the leading behaviour of the non-divergent part $U_+(\frac{D-1}{2}, \frac{D}{2} + 1, \epsilon\kappa^2)$ of the $\epsilon\kappa$-expansion of $U(\frac{D-1}{2}, \frac{D}{2} + 1, \epsilon\kappa^2)$ is a constant term [49,50]

$$U_+\left(n, n + \frac{3}{2}, \epsilon\kappa^2\right) = -\frac{\Gamma(-n-\frac{1}{2})}{2\sqrt{\pi}} + \mathcal{O}(\epsilon\kappa^2), \tag{2.23}$$

whereas in the even case $D = 2n$ there is a leading logarithmically divergent term [49,50]

$$U_+\left(n - \frac{1}{2}, n + 1, \epsilon\kappa^2\right)$$
$$= \frac{(-1)^n}{2\sqrt{\pi}\,\Gamma(n+1)}\left(\psi(n - 1/2) - \psi(n + 1) + \gamma + \log(\epsilon\kappa^2)\right) + \mathcal{O}(\epsilon\kappa^2), \tag{2.24}$$

$\psi(s) = \frac{\Gamma'(s)}{\Gamma(s)}$ being the digamma function and γ the Euler constant.

One important fact is that there are no cancellations in the expression (2.15) between subleading asymptotic terms $\mathcal{O}(\epsilon\kappa_i^2)$ of the confluent hypergeometric function $U(n - \frac{1}{2}, n + 1, \epsilon\kappa_i^2)$ and divergent contributions coming from the remaining sum over the eigenvalues κ_i; nor between divergent terms of $U(n - \frac{1}{2}, n + 1, \epsilon\kappa_i^2)$ and subleading $\mathcal{O}(\epsilon)$ terms of the sums over κ_i.

In summary, the Casimir energy arises only from the product of the finite $\mathcal{O}(1)$ terms of (2.23) and (2.24) which correspond to two different types of behaviours.

2.1. Odd-dimensional $D = 2n + 1$ spaces

In this case the Casimir energy (2.22) can be obtained from formula (2.21) keeping only the leading asymptotic contributions (2.23) of the confluent hypergeometric function $U(\frac{D-1}{2}, \frac{D}{2} + 1, \epsilon k^2)$. The result is given by the following contour integral of the spectral function

$$\frac{c_U^{(2n+1)}}{L^{2n+1}} = \frac{(-1)\Gamma(-\frac{2n+1}{2})L_0^{2n+1}}{(4\pi)^{\frac{2n+1}{2}}(L^{2n+1} - L_0^{2n+1})} \lim_{\epsilon \to 0} \frac{1}{2\pi i} \oint dk\, k^{2n+1} e^{-\epsilon k^2}$$
$$\times \left[(L_0 - L)\frac{k - k^*}{|k - k^*|} - \frac{d}{dk}\log\left(\frac{h_U^{(L)}(k)}{h_U^{(L_0)}(k)}\right)\right]. \tag{2.25}$$

Since this expression is finite and convergent in the $\epsilon \to 0$ limit, we can drop the regulating exponential heat kernel factor $e^{-\epsilon k^2}$. In this case, because of the holomorphic properties of the integrand, the integration can also be extended to the contour given by an infinite semi-circle limited in its left-hand side by the imaginary axis. As long as the integration over the semicircle is zero, the integration is reduced to the imaginary axis of the complex k-plane, and taking into account the parity invariance of the integrand the integration range can be reduced to the positive imaginary axis. The final integral expression for the Casimir energy is

$$\frac{c_U^{(2n+1)}}{L^{2n+1}} = \frac{4(-1)^n\Gamma(-\frac{2n+1}{2})L_0^{2n+1}}{(4\pi)^{\frac{2n+3}{2}}(L^{2n+1} - L_0^{2n+1})} \int_0^\infty dk\, k^{2n+1}\left[L - L_0 - \frac{d}{dk}\log\left(\frac{h_U^{(L)}(ik)}{h_U^{(L_0)}(ik)}\right)\right]. \tag{2.26}$$

2.2. Even-dimensional $D = 2n$ spaces

The even case presents some further interesting peculiarities. Following the analysis of the odd case, but taking into account the different asymptotic behaviour (2.24) of the confluent hypergeometric function $U_+(n - \frac{1}{2}, n + 1, \epsilon \kappa^2)$, we obtain the Casimir energy in terms of the contour integral

$$\frac{c_U^{(2n)}}{L^{2n}} = \frac{(-1)^n (4\pi)^{-n} L_0^{2n}}{\Gamma(n+1)(L^{2n} - L_0^{2n})} \lim_{\epsilon \to 0} \frac{1}{2\pi i} \oint dk \, k^{2n} \left[(L_0 - L) \frac{k}{|k|} - \frac{d}{dk} \log \frac{h_U^{(L)}(k)}{h_U^{(L_0)}(k)} \right]$$
$$\times \left(\psi \left(n - \frac{1}{2} \right) - \psi(n+1) + \gamma + \log(\epsilon \kappa^2) \right) e^{-\epsilon k^2}.$$

The exponential factor of the heat kernel can again be dropped and the integration reduced to an integral over the imaginary axis. But in this case the terms proportional to $\psi(n - \frac{1}{2}) - \psi(n+1) + \gamma$ are parity odd and the integral over the positive and negative imaginary axes cancel each other. Only the terms proportional to the logarithm term $\log(\epsilon \kappa_i^2)$ provide a non-vanishing contribution. Due to the existence of a branch cut that we fix along the real positive axis the contribution of positive imaginary axis picks up a factor $i\pi/2$ whereas in the negative imaginary axis this factor is $-i\pi/2$. The total contribution of the integral reduces to a very compact finite formula

$$\frac{c_U^{(2n)}}{L^{2n}} = -\frac{(4\pi)^{-n} L_0^{2n}}{\Gamma(n+1)(L^{2n} - L_0^{2n})} \int_0^\infty dk \, k^{2n} \left[L - L_0 - \frac{d}{dk} \log \left(\frac{h_U^{(L)}(ik)}{h_U^{(L_0)}(ik)} \right) \right] \qquad (2.27)$$

for the calculation of the Casimir energy.

Expressions (2.26) and (2.27) allow the calculation of Casimir energy for arbitrary consistent boundary conditions in the parallel plates configuration in any spatial dimension. We restrict our analysis to the two most interesting cases from physical point of view: massless scalar theories in $(2+1)$- and $(3+1)$-dimensional spacetimes (the case $1+1$ has been already analysed from this viewpoint in Refs. [23,24]). What is interesting about these two cases is that many of the new boundary conditions of the parallel plates can be implemented in the laboratory and the theoretical results falsified.

3. Casimir energy in three dimensions

In the most realistic three-dimensional $(D = 3)$ case the Casimir energy is given by the integral

$$\frac{E_U^{(3)}}{S} = \frac{c_U^{(3)}}{L^3} = \frac{-L_0^3}{6\pi^2(L^3 - L_0^3)} \int_0^\infty dk \, k^3 \left[L - L_0 - \frac{d}{dk} \log \left(\frac{h_U^{(L)}(ik)}{h_U^{(L_0)}(ik)} \right) \right], \qquad (3.1)$$

for any type of consistent boundary conditions (i.e. $U \in \mathcal{M}_F$).

In many cases the calculation of the Casimir energy using the spectral formula (3.1) can be achieved analytically but in general it requires the use of numerical simulations. Let us first compare the analytic results obtained by the spectral function method and the results obtained by other methods (e.g. zeta function regularisation [36,38,40,41]).

3.1. Periodic boundary conditions

They correspond to a folding of the space into a cylinder, $\psi(0) = \psi(L)$, $\psi'(0) = \psi'(L)$, and are described by the unitary operator

$$U_p = \sigma_1 = \begin{pmatrix} 0 & 1 \\ 1 & 0 \end{pmatrix}. \tag{3.2}$$

The associated spectral function,

$$h_p^{(L)}(k) = 4k(\cos kL - 1), \tag{3.3}$$

reduces the integrand in expression (3.1) to

$$L - L_0 - \frac{d}{dk}\left(\log\frac{h_p^{(L)}(ik)}{h_p^{(L_0)}(ik)}\right) = L - L_0 + L_0 \coth\frac{kL_0}{2} - L \coth\frac{kL}{2},$$

and the Casimir energy is, thus, given by

$$\frac{E_p^{(3)}}{S} = \frac{c_p^{(3)}}{L^3} = \frac{-L_0^3}{6\pi^2(L^3 - L_0^3)} \int\limits_0^\infty dk\, k^3 \left[L - L_0 + L_0 \coth\left(\frac{kL_0}{2}\right) - L\coth\left(\frac{kL}{2}\right)\right]$$

which, can be analytically integrated out, giving rise to a negative Casimir energy, that agrees with results obtained by other standard methods (e.g. zeta function regularisation [40]).

$$\frac{E_p^{(3)}}{S} = -\frac{\pi^2}{45L^3}. \tag{3.4}$$

As it is well known the Casimir effect in the periodic case introduces an attractive force which tends to shrink the cylinder.

3.2. Dirichlet boundary condition

In this case $\psi(0) = \psi(L) = 0$, the unitary operator is $U_d = -\mathbb{I}$, and the associated spectral function is

$$h_d^{(L)}(k) = 4i\sin kL. \tag{3.5}$$

The Casimir energy is given by the well-known Casimir result

$$\frac{E_d^{(3)}}{S} = \frac{-L_0^3}{6\pi^2(L^3 - L_0^3)} \int\limits_0^\infty dk\, k^3 \left[L - L_0 + L_0 \coth(kL_0) - L\coth(kL)\right] = -\frac{\pi^2}{720L^3},$$

which again is negative and $\frac{1}{16}$ times smaller than the periodic case.

3.3. Neumann boundary condition

In this case, $\psi'(0) = \psi'(L) = 0$, the associated unitary operator is $U_n = \mathbb{I}$, and its spectral function

$$h_n^{(L)}(k) = 4ik^2 \sin kL. \tag{3.6}$$

Although the spectral function $h_n(k)$ is different from $h_d^{(L)}(k)$, the result is the same as for Dirichlet boundary conditions

$$\frac{E_n^{(3)}}{S} = -\frac{\pi^2}{720L^3}.$$ (3.7)

In both cases, Dirichlet and Neumann, the character of the Casimir force between plates is attractive, and $\frac{1}{16}$ times smaller than in the periodic case.

3.4. Anti-periodic boundary conditions

They correspond to $\psi(0) = -\psi(L)$, $\psi'(0) = -\psi'(L)$, and are described by the unitary operator

$$U_{ap} = -\sigma_1 = \begin{pmatrix} 0 & -1 \\ -1 & 0 \end{pmatrix}.$$ (3.8)

The associated spectral function,

$$h_{ap}^{(L)}(k) = 4k(\cos kL + 1),$$ (3.9)

reduces the integrand in expression (3.1) to

$$L - L_0 + L_0 \tanh\left(\frac{kL_0}{2}\right) - L \tanh\left(\frac{kL}{2}\right).$$

In the case of anti-periodic boundary conditions the Casimir energy

$$\frac{E_{ap}^{(3)}}{S} = \frac{-L_0^3}{6\pi^2(L^3 - L_0^3)} \int_0^\infty dk\, k^3 \left[L - L_0 + L_0 \tanh\left(\frac{kL_0}{2}\right) - L \tanh\left(\frac{kL}{2}\right)\right] = \frac{7\pi^2}{360L^3}$$

is positive, which corresponds to a repulsive Casimir force between plates.

3.5. Zaremba boundary condition

There are two special boundary conditions which are Neumann at one boundary and Dirichlet at the other, or vice versa. The unitary matrices are

$$U_Z = \pm\sigma_3 = \pm \begin{pmatrix} 1 & 0 \\ 0 & -1 \end{pmatrix},$$

their spectral function

$$h_Z(k) = -8k \cos kL$$ (3.10)

and the corresponding Casimir energy

$$\frac{E_Z^{(3)}}{S} = \frac{-L_0^3}{6\pi^2(L^3 - L_0^3)} \int_0^\infty dk\, k^3 \left[L - L_0 + L_0 \tanh(kL) - L \tanh(kL)\right] = \frac{7\pi^2}{5760L^3},$$

is positive which corresponds to a repulsive Casimir force between the parallel plates.

3.6. Quasi-periodic boundary conditions

This is a one-parameter family of boundary conditions defined by

$$\psi(L) = \tan\frac{\alpha}{2}\,\psi(0), \qquad \psi'(L) = \cot\frac{\alpha}{2}\,\psi'(0),$$

with unitary operator

$$U_{qp} = \cos\alpha\,\sigma_3 + \sin\alpha\,\sigma_1, \quad \alpha \in [-\pi/2, \pi/2].\tag{3.11}$$

The associated spectral function is

$$h_{qp}^{(L)}(k) = 4k(\cos kL - \sin\alpha),\tag{3.12}$$

and the Casimir energy is given by the following integral expression

$$\frac{E_{qp}^{(3)}}{S} = \frac{-L_0^3}{6\pi^2(L^3 - L_0^3)}\int_0^\infty dk\,k^3\left[L - L_0 + \frac{L_0\sinh(kL_0)}{\sin(\alpha) - \cosh(kL_0)} - \frac{L\sinh(kL)}{\sin(\alpha) - \cosh(kL)}\right],$$

$$\tag{3.13}$$

which gives

$$c_{qp}^{(3)} = -\frac{1}{\pi^2}\left(\mathrm{li}_4\!\left(-ie^{i\alpha}\right) + \mathrm{li}_4\!\left(ie^{-i\alpha}\right)\right),\tag{3.14}$$

where

$$\mathrm{li}_n(z) \equiv \frac{(-1)^{n-1}}{(n-2)!}\int_0^1 \frac{dt}{t}\log(1-zt)\log^{n-2}(t) = \sum_{j=1}^\infty \frac{z^j}{j^n}$$

denotes the integral logarithm function. The combination of integral logarithms $\mathrm{li}_4(-ie^{i\alpha}) + \mathrm{li}_4(ie^{-i\alpha})$ can be reduced to a fourth order polynomial in α for $\alpha \in [-\pi/2, \pi/2])$, thus the Casimir energy coefficient $c_{qp}^{(3)}$ is given by

$$c_{qp}^{(3)} = \frac{7\pi^2}{5760} - \frac{\pi\alpha}{16} - \frac{\alpha^2}{48} + \frac{\alpha^3}{12\pi} + \frac{\alpha^4}{24\pi^2}, \quad \alpha \in [-\pi/2, \pi/2].\tag{3.15}$$

The behaviour of the coefficient $c_{qp}^{(3)}$ of the Casimir energy as a function of α in the interval $[-\pi/2, \pi/2]$ shows that there is a value $\alpha_0^{(qp)}$ of α where the Casimir energy and the Casimir force between plates vanish. This special value

$$\alpha_0^{(qp)} = \pi\left(-\frac{1}{2} + \sqrt{1 - 2\sqrt{\frac{2}{15}}}\right)\tag{3.16}$$

corresponds to the splitting point between attractive and repulsive regimes. For $-\pi/2 \leqslant \alpha < \alpha_0^{(qp)}$ the Casimir energy is positive and hence the Casimir force between plates has a repulsive character, and when $\pi/2 \geqslant \alpha > \alpha_0^{(qp)}$, the Casimir force between plates becomes attractive, corresponding to a negative Casimir energy.

3.7. Pseudo-periodic boundary conditions

Pseudo-periodic boundary conditions are a family of one-parameter family of boundary conditions that generalise periodic and anti-periodic conditions, i.e.

$$\psi(L) = e^{-i\alpha}\psi(0), \qquad \psi'(L) = e^{-i\alpha}\psi'(0).$$

The unitary matrices defining the boundary conditions of this family are

$$U_{pp} = \cos\alpha\,\sigma_1 - \sin\alpha\,\sigma_2 = \begin{pmatrix} 0 & e^{i\alpha} \\ e^{-i\alpha} & 0 \end{pmatrix}, \quad \alpha \in [-\pi, \pi], \tag{3.17}$$

and their spectral functions read

$$h_{pp} = 4k(\cos kL - \cos\alpha). \tag{3.18}$$

The calculation of Casimir energy

$$\frac{E_{pp}^{(3)}}{S} = \frac{-L_0^3}{6\pi^2(L^3 - L_0^3)} \int\limits_0^\infty \left[L - L_0 - \frac{L\sinh(kL)}{\cosh(kL) - \cos(\alpha)} - \frac{L_0\sinh(kL_0)}{\cosh(kL_0) - \cos(\alpha)} \right] k\,dk$$

can be reduced to that of the quasi-periodic boundary conditions case by replacing α_{qp} with $\alpha_{pp} + \pi/2$, i.e.

$$c_{pp}^{(3)}(\alpha) = -\frac{\pi^2}{45} + \frac{\alpha^2}{6} - \frac{|\alpha|^3}{6\pi} + \frac{\alpha^4}{24\pi^2}, \quad \alpha \in [-\pi, \pi]. \tag{3.19}$$

There are two values of α where the Casimir energy and Casimir force between plates vanish

$$\alpha_{0\pm}^{(pp)} = \mp\pi\left(1 - \sqrt{1 - 2\sqrt{\frac{2}{15}}}\right). \tag{3.20}$$

For $\alpha_{0-}^{(pp)} < \alpha < \alpha_{0+}^{(pp)}$ the Casimir energy is negative, which leads to an attractive Casimir force between plates. However, for $-\pi < \alpha < \alpha_{0-}^{(pp)}$ or $\alpha_{0+}^{(pp)} < \alpha < \pi$, the Casimir energy is positive, and the force between plates is repulsive.

3.8. Robin boundary conditions

The one-parameter family of Robin boundary conditions

$$\psi'(0) = \tan\frac{\alpha}{2}\,\psi(0), \qquad \psi'(L) = \tan\frac{\alpha}{2}\,\psi(L),$$

is characterised by the family of unitary matrices $U_r = e^{i\alpha}\mathbb{I}$, with $\alpha \in [0, \pi]$ and spectral function

$$h_{U_r}^{(0)}(k) = 2ie^{i\alpha}\left(-2k\sin\alpha\cos kL + \left(k^2 - 1 + \left(k^2 + 1\right)\cos\alpha\right)\sin kL\right).$$

In this case it is not possible to find an analytical expression for the Casimir energy $c_r^{(3)}$, thus one has to proceed numerically from expression (3.1). The Casimir energy for Robin boundary conditions is displayed in Fig. 2 which is in agreement with previous analyses [51,52]. Of note is that $c_r^{(3)}$ is negative for all values of $\alpha \in [0, \pi/2]$. In other words, the Casimir force between plates in this case is always attractive, which is in agreement with the Kenneth–Klich theorem (see below).
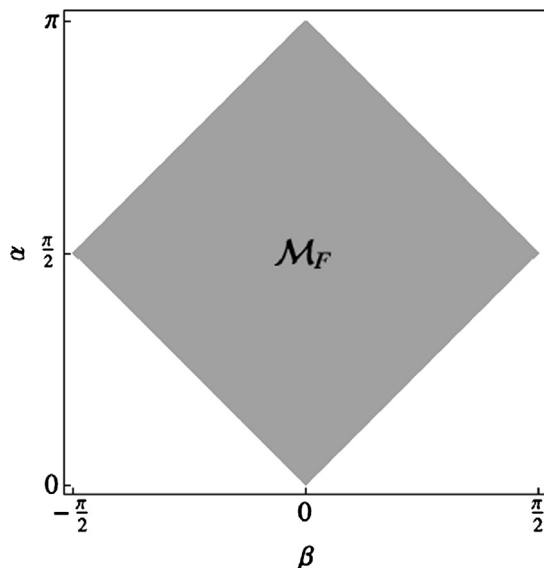
Fig. 1. Rhombic slice of the space of consistent boundary conditions $\mathcal{M}_F$ for a scalar field theory confined between two homogeneous parallel plates in the α–β planes for fixed value of $\mathbf{n}$ and $0 < \alpha \pm \beta < \pi$. The conical structure of the full space $\mathcal{M}_F$ of boundary conditions is clearly inferred from the displayed rhombus.

3.9. Pauli matrices boundary conditions

Another case of special interest are the boundary conditions that are located at left and right corners of the rhombus of Fig. 1, i.e. boundary conditions corresponding to points on the unit sphere S^2 for values $\alpha = \pm\beta = \frac{\pi}{2}$, i.e. $U_\mathbf{n} = \mathbf{n} \cdot \boldsymbol{\sigma}$. These two-parameter family of boundary conditions includes periodic, anti-periodic, quasi-periodic and pseudo-periodic boundary conditions. The Casimir energy given by

$$\frac{E(n_1)}{S} = \frac{1}{L^3}\left(-\frac{\pi^2}{45} + \frac{(\arccos n_1)^2}{6} - \frac{(\arccos n_1)^3}{6\pi} + \frac{(\arccos n_1)^4}{24\pi^2}\right), \tag{3.21}$$

with $\arccos n_1 \in [0, 2\pi]$, has two regimes, attractive and repulsive, separated by a one-dimensional circle of Casimirless boundary conditions (see Fig. 3) given by $\alpha = \beta = \frac{\pi}{2}$ and

$$n_1 = \cos\pi\left[1 \pm (1 - 2\sqrt{2/15})^{\frac{1}{2}}\right]. \tag{3.22}$$

It is remarkable that all analytical results obtained by the spectral function method agree with those obtained by other methods like zeta function regularisation method. However the expression for the Casimir energy in terms of a contour integral of the spectral function provides a very efficient method for numerical calculations of the Casimir energy in the cases where it cannot be achieved by analytic methods.

In this way we can calculate the Casimir energy for a wider class of boundary conditions using the spectral function method (3.1). In many cases these results were previously known, and the results obtained by the spectral function method are in perfect agreement with those found in the literature. Apart from the well-known analytic results described above there is also
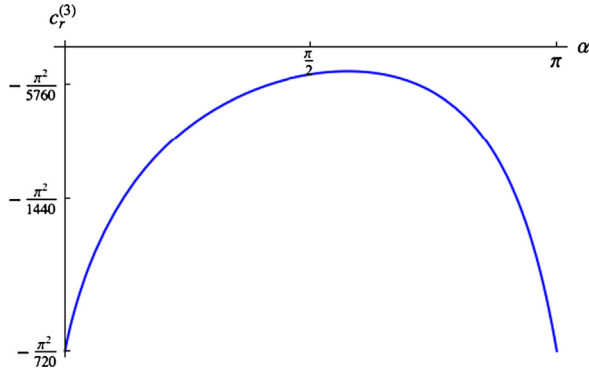
Fig. 2. α-dependence of the $c_r^{(3)}$ coefficient of Casimir energy for Robin boundary conditions for $\alpha \in [0, \pi]$.
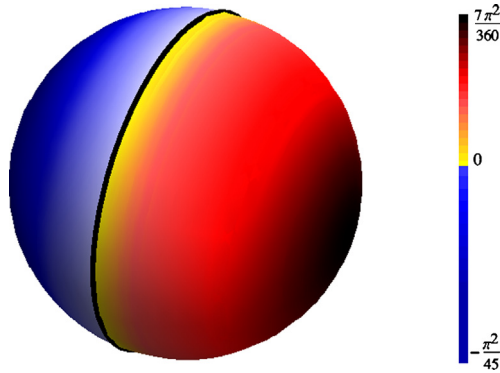

Fig. 3. (Colour online.) Variation of the $c_U^{(3)}$ coefficient of the Casimir energy in the consistency region $\beta = \frac{\pi}{2}$, $\alpha = \frac{-\pi}{2}$ for any value of the normal vector $\mathbf{n}$. The black curve correspond to boundary conditions with vanishing Casimir energy and blue (red) regions to boundary conditions with attractive (repulsive) Casimir forces.

agreement with the numerical simulations of cases like Robin boundary conditions where there are not analytic expressions for the Casimir energy [51,52].

4. Casimirless boundary conditions

For generic boundary conditions there are not analytic results but the efficiency of the numerical analysis using formula (3.1) allows the calculation of the Casimir energy for any boundary condition in one simple step. The space of boundary conditions $\mathcal{M}_F$ is four-dimensional, however, the Casimir energy only depends on three parameters α, β, n_1, i.e. it is independent of the value of n_2, n_3 components of the unitary vector $\mathbf{n} = (n_1, n_1, n_3)$. Hence a global calculation of Casimir energy reduces to the calculation of a family of planar functions on slices of $\mathcal{M}_F$ parametrised by the different values of $n_1 \in [-1, 1]$. In each slice the Casimir energy can be represented by its contour lines and this makes the identification of the attractive and repulsive regimes easier by highlighting the curves where the Casimir energy vanishes.

In this representation there are redundancies because some points in the slices n_1 and $-n_1$ correspond to the same boundary conditions. For this a reason we only consider positive values of n_1.
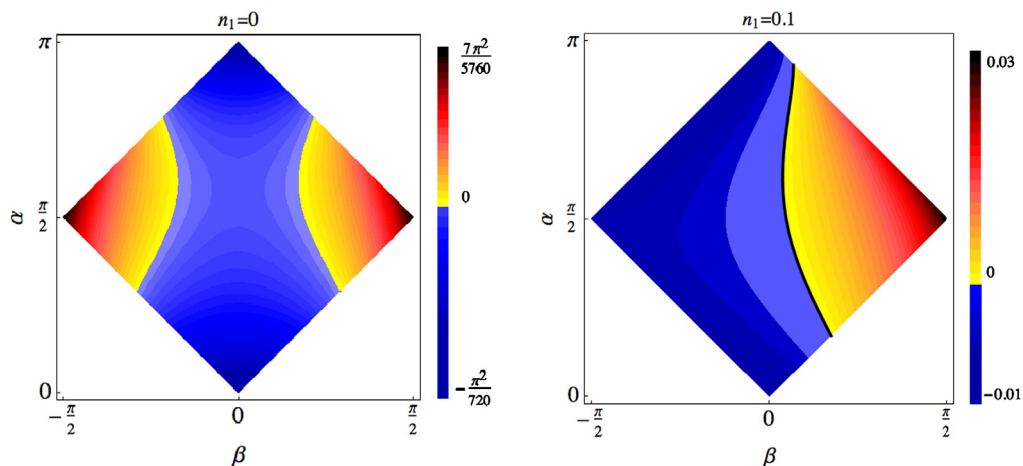
Fig. 4. (Colour online.) Variation of the $c^{(3)}$ coefficient of the Casimir energy in the consistency domain of boundary conditions $|\beta| < \alpha < \pi - |\beta|$, for $n_1 = 0$ and $n_1 = 0.1$. Black curves correspond to boundary conditions with vanishing Casimir energy and blue (red) regions correspond to boundary conditions with negative (positive) values of Casimir energy.
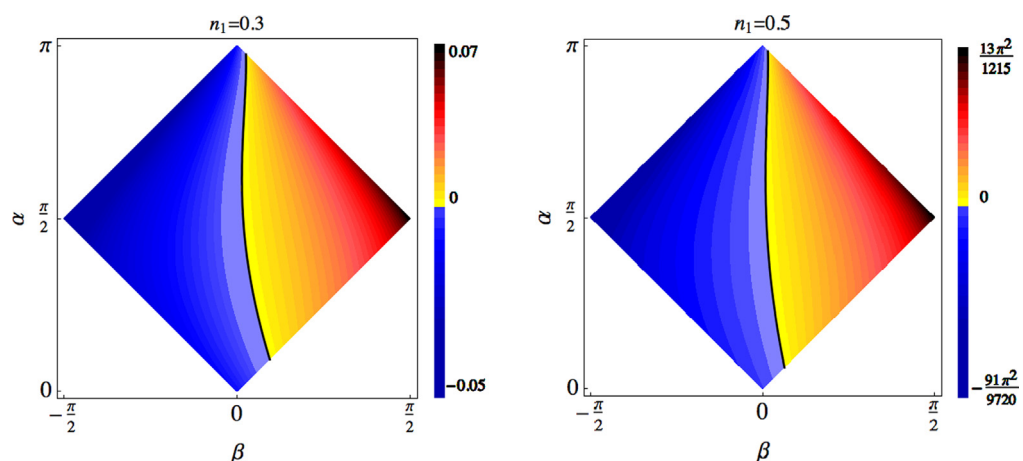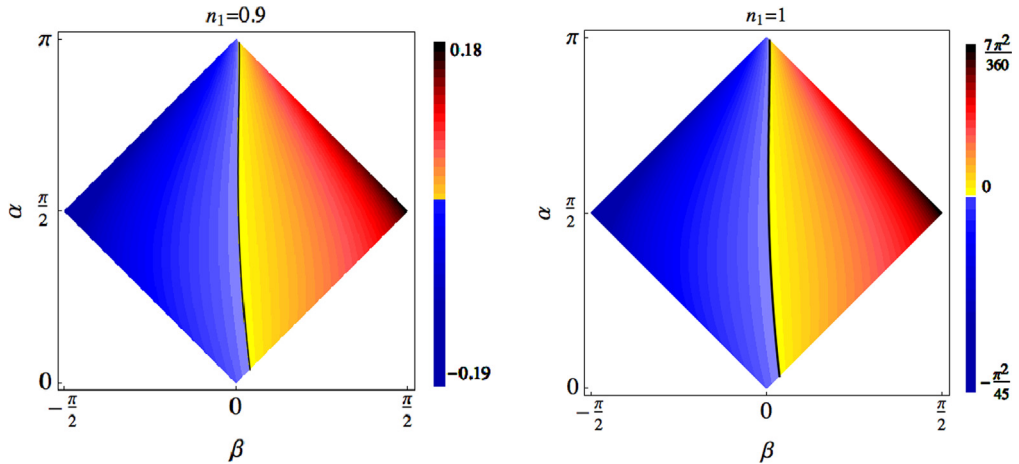

Fig. 5. (Colour online.) Variation of the $c^{(3)}$ coefficient of the Casimir energy in the consistency domain of boundary conditions $|\beta| < \alpha < \pi - |\beta|$, for $n_1 = 0.3$ and $n_1 = 0.5$. Black curves correspond to boundary conditions with vanishing Casimir energy and blue (red) regions correspond to boundary conditions with negative (positive) values of Casimir energy.

The results show that Casimir energy, as a function $c_U^{(3)}/L^3 : \mathcal{M}_F \to \mathbb{R}$, has negative, positive and null values (see Figs. 4–6). These correspond to attractive, repulsive, and zero Casimir effect, i.e., there are operators $U \in \mathcal{M}_F$ which give rise to field theories without Casimir effect (zero Casimir energy). Such boundary conditions are characterised by the solutions of the equation

$$\int_0^\infty dk k^3 \left[L - L_0 - \frac{d}{dk} \log\left(\frac{h_U^{(L)}(ik)}{h_U^{(L_0)}(ik)} \right) \right] = 0 \tag{4.1}$$

Fig. 6. (Colour online.) Variation of the $c^{(3)}$ coefficient of the Casimir energy in the consistency domain of boundary conditions $|\beta| < \alpha < \pi - |\beta|$, for $n_1 = 0.9$ and $n_1 = 1$. Black curves correspond to boundary conditions with vanishing Casimir energy and blue (red) regions correspond to boundary conditions with negative (positive) values of Casimir energy.

in $\mathcal{M}_F$. Eq. (4.1) has infinite solutions in $\mathcal{M}_F$ as can be seen from Figs. 4–6. Null Casimir energy subspaces are 3-dimensional and their co-dimension is 1 because they only satisfy one equation constraint (4.1).

The most relevant property of the 3-dimensional subspace of Casimirless boundary conditions is that it splits the space of physical boundary conditions $\mathcal{M}_F$ into two disjoint subsets: one containing all boundary conditions that generate repulsive Casimir force and the other containing those with attractive Casimir force. In other words the existence of Casimirless boundary conditions highlights the transition between both types of regimes. Although the subspace of boundary conditions with vanishing Casimir energy is connected, in some slices the intersection of the subspace defined by (4.1) has two connected components curves while for others it has only one connected component.

The numerical results show that the minimum of Casimir energy is obtained with periodic boundary conditions, which means that these boundary conditions generate the strongest attractive Casimir force between the plates. In the same way we find that the maximum value of Casimir energy is obtained with anti-periodic boundary conditions, which means that these boundary conditions generate the strongest repulsive Casimir force.

Using the numeric calculations above we can verify that the Kenneth–Klich theorem [14] also holds in $3+1$ dimensions. The theorem states that the Casimir force between two identical bodies is always attractive. It is implicit in the assumptions of the theorem that the boundary conditions introduced by the two bodies are each other independent. The only conditions that satisfy this property are those with $n_1 = n_2 = 0, n_3 = 1$, i.e.

$$U(\alpha, \beta, (0, 0, 1)) = e^{i\alpha}(\cos\beta\, \mathbb{I} + i\sigma_3 \sin\beta) = \begin{pmatrix} e^{i(\alpha+\beta)} & 0 \\ 0 & e^{i(\alpha-\beta)} \end{pmatrix}. \qquad (4.2)$$

Boundary conditions which modelling identical bodies require $\beta = 0$ and in this case we have identical Robin boundary conditions with $n_1 = 0$ which corresponds to boundary conditions sitting on the vertical line connecting the Dirichlet and Neumann corners of the rhombus in

Fig. 1. In fact the above results show that the same behaviour hold for bodies with slightly different boundary conditions. This follows from the continuity of the Casimir energy in the space of boundary conditions $\mathcal{M}_F$. The repulsive behaviour requires in general a rather different boundary conditions for the two plates, e.g. Zaremba boundary conditions ($\alpha = \pm\beta = \frac{\pi}{2}$, i.e. $U = \pm\sigma_3$) located on the left (right) corners of the rhombus which correspond to two plates, one with Neumann boundary conditions whereas the other has Dirichlet boundary conditions.

The same behaviour appears for higher-dimensional $D + 1$ field theories. In these cases the Casimir energy for identical plates is given by

$$\frac{c_r^{(2n+1)}}{L^{2n+1}} = \frac{(-1)^n (4\pi)^{-\frac{2n+1}{2}} \Gamma(-\frac{2n+1}{2}) L_0^{2n+1}}{\pi(L^{2n+1} - L_0^{2n+1})}$$
$$\times \int_0^\infty dk\, k^{2n+1} \left[L - L_0 - \frac{d}{dk} \log\left(\frac{h_r^{(L)}(ik)}{h_r^{(L_0)}(ik)} \right) \right] \tag{4.3}$$

for $D = 2n + 1$ odd dimensions, or

$$\frac{c_r^{(2n)}}{L^{2n}} = -\frac{(4\pi)^{-n} L_0^{2n}}{\Gamma(n+1)(L^{2n} - L_0^{2n})} \int_0^\infty dk\, k^{2n} \left[L - L_0 - \frac{d}{dk} \log\left(\frac{h_r^{(L)}(ik)}{h_r^{(L_0)}(ik)} \right) \right] \tag{4.4}$$

for $D = 2n$ even dimensions. Since $(-1)^n \Gamma(-\frac{2n+1}{2})$ is always negative it is sufficient to prove that the integrand is in both cases is a positive function of k. Boundary conditions introduced by two independent identical bodies are given by (4.2) with $\beta = 0$. The associated spectral function is

$$h_r^{(L)}(ik) = 2e^{i\alpha} \left(\left(k\cos\frac{\alpha}{2} + \sin\frac{\alpha}{2} \right)^2 e^{kL} - \left(k\cos\frac{\alpha}{2} - \sin\frac{\alpha}{2} \right)^2 e^{-kL} \right), \tag{4.5}$$

and

$$\frac{h_r^{(L)\prime}(ik)}{h_r^{(L)}(ik)} = \frac{4k\cos^2\frac{\alpha}{2}\sinh kL + 2\sin\alpha\cosh kL + L(k\cos\frac{\alpha}{2} + \sin\frac{\alpha}{2})^2 e^{kL} + L(k\cos\frac{\alpha}{2} - \sin\frac{\alpha}{2})^2 e^{-kL}}{(k\cos\frac{\alpha}{2} + \sin\frac{\alpha}{2})^2 e^{kL} - (k\cos\frac{\alpha}{2} - \sin\frac{\alpha}{2})^2 e^{-kL}}. \tag{4.6}$$

When $L > L_0$ the inequality

$$h_r^{(L)\prime}(ik)/h_r^{(L)}(ik) - h_r^{(L_0)\prime}(ik)/h_r^{(L_0)}(ik) < L - L_0 \tag{4.7}$$

provides the necessary bound which ensures that the integral is always positive. Thus in any dimension the Casimir energy is always negative

$$c_r^D < 0$$

as required by Kenneth–Klich theorem.

5. Casimir energy in 2 dimensions

Two-dimensional systems have acquired recent interest since the appearance of new materials like graphene and new physical effects which are specific of two-dimensional systems like the quantum Hall effects. On the other hand, as we have shown the calculation of Casimir effect presents some subtleties in even-dimensional spaces. In the $D = 2$ case the integral for transverse modes apparently presents logarithmic divergences for all the orders in the power expansion of parameter ϵ. Some of them have been analysed in the literature, see Refs. [7,53,40,54,8]. However, it is remarkable that these divergences disappear, as we have shown in the preceding section, giving rise to a finite univocally defined Casimir energy and a finite Casimir pressure on the plates proportional to the cubic power of the inverse distance between plates. The Casimir energy in this case is given by

$$\frac{c_U^{(2)}}{L^2} = -\frac{1}{4\pi} \frac{L_0^2}{L^2 - L_0^2} \int_0^\infty dk \, k^2 \left[L - L_0 - \frac{d}{dk} \log\left(\frac{h_U^{(L)}(ik)}{h_U^{(L_0)}(ik)} \right) \right]. \tag{5.1}$$

In some cases the integral (5.1) can be analytically evaluated, e.g. for Dirichlet/Neumann boundary conditions we get

$$c_d^{(2)} = c_n^{(2)} = -\frac{\zeta(3)}{8\pi},$$

whereas we have

$$c_p^{(2)} = -\frac{\zeta(3)}{\pi}, \qquad c_{ap}^{(2)} = \frac{3\zeta(3)}{4\pi}, \qquad c_z^{(2)} = \frac{3\zeta(3)}{32\pi},$$

for periodic, anti-periodic and Zaremba boundary conditions. The results are finite and in agreement with those obtained using other methods such as zeta function regularisation method [7,53, 40,54,8].

We also obtain analytic expressions for the Casimir energy for quasi-periodic (3.11) and pseudo-periodic (3.17) boundary conditions

$$c_{qp}^{(2)} = -\frac{1}{2\pi} \left(\mathrm{li}_3\left(-i e^{i\alpha}\right) + \mathrm{li}_3\left(i e^{-i\alpha}\right) \right), \quad \alpha \in [-\pi/2, \pi/2], \tag{5.2}$$

$$c_{pp}^{(2)} = -\frac{1}{2\pi} \left(\mathrm{li}_3\left(e^{i\alpha}\right) + \mathrm{li}_3\left(e^{-i\alpha}\right) \right), \quad \alpha \in [-\pi, \pi], \tag{5.3}$$

although in these cases the α-dependence of the Casimir energy is not polynomial unlike in $3 + 1$ dimensions (see Section 3).

The results explicitly show the universal character of the Casimir energy, even for $(2 + 1)$-dimensional spacetimes where some authors suggested the presence of logarithmic divergences which would make the Casimir phenomenon dependent on the regularisation method and the renormalisation scheme. We have demonstrated by using a heat kernel regularisation the absence of these divergences and proved the universal character of the Casimir energy between plates for any even-dimensional space.

In $2 + 1$ dimensions there are also boundary conditions that generate attractive and repulsive Casimir effects as in $3 + 1$ dimensions. In the interface between both regimes there are boundary conditions that do not generate any Casimir force. Those boundary conditions of $\mathcal{M}_F$ with vanishing Casimir energy are characterised as the solutions of equation
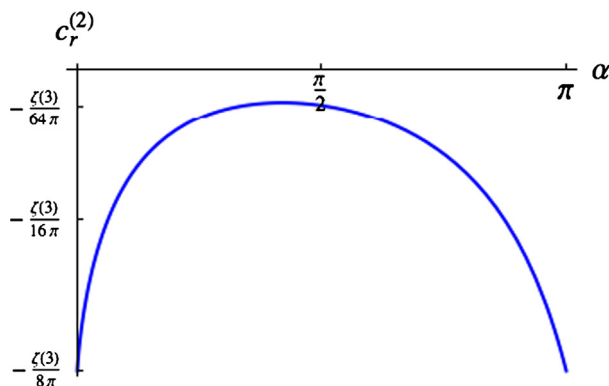
Fig. 7. Variation of the $c_U^{(2)}$ coefficient of the Casimir energy as a function of $\alpha \in [-\pi, \pi]$ for Robin boundary conditions.

$$\int_0^\infty k^2 \left[L - L_0 - \frac{d}{dk} \log\left(\frac{h_U^{(L)}(ik)}{h_U^{(L_0)}(ik)} \right) \right] dk = 0, \tag{5.4}$$

in $\mathcal{M}_F$.

In particular, Casimirless boundary conditions arise in the one-parameter families of quasi-periodic and pseudo-periodic boundary conditions where the Casimir energies given by (5.2) and (5.3) point out the existence of three values of the α parameter for which the coefficient $c_U^{(2)}$ vanishes (see Fig. 11). They correspond to Casimirless boundary conditions.

In contrast, for Robin boundary conditions the numerical result is displayed in Fig. 7 show that the Casimir energy is always negative for any value of $\alpha \in [0, \pi/2]$. In other words, in this case the Casimir force between plates is always attractive.

Finally, using Eq. (5.1) the behaviour of $c_U^{(2)}$ can be numerically evaluated in the whole domain $\mathcal{M}_F$ of consistent boundary conditions. Figs. 10, 9 and 8 show contour plots of $c_U^{(2)}$ for different values of parameter n_1.

Again it is explicitly shown that for any value of n_1 there are curves of boundary conditions with vanishing Casimir energy (thick lines). For the rest of boundary conditions in $\mathcal{M}_F$ the Casimir energy can take positive and negative values, which correspond to repulsive or attractive Casimir forces between the plates.

The results also confirm the behaviour inferred from the Kenneth–Klich theorem in $2 + 1$ dimensions. Indeed the Casimir force between two identical wires in $2 + 1$ dimensions is always attractive as corresponds to the case of two identical Robin boundary conditions. This behaviour of the Casimir force is not exclusive of bodies with identical Robin boundary conditions, i.e. $\beta = n_1 = 0$ but also for bodies with slightly different Robin boundary conditions. This follows from the continuity of the Casimir energy in the space of boundary conditions $\mathcal{M}_F$ and demonstrates that the repulsive character of Casimir force can only appear for bodies with very different boundary conditions e.g. mixed Dirichlet–Neumann conditions as in Zaremba boundary conditions.

6. Discussion and conclusions

From the global analysis of the dependence of Casimir energy on the type of boundary conditions performed throughout this paper we can extract some consequences of physical interest.
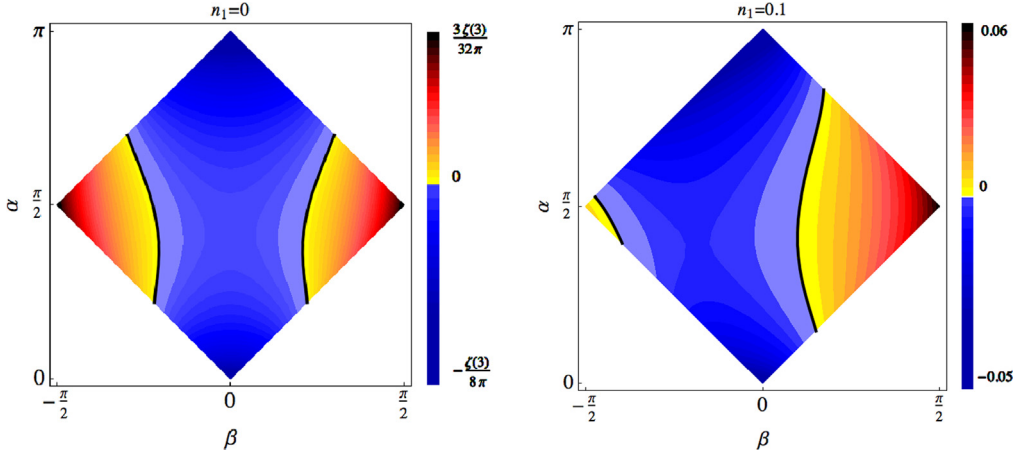
Fig. 8. (Colour online.) Variation of the $c^{(2)}$ coefficient of the Casimir energy in the consistency domain of boundary conditions $|\beta| < \alpha < \pi - |\beta|$ for $n_1 = 0$ and $n_1 = 0.1$. Black curves correspond to boundary conditions with vanishing Casimir energy and blue (red) regions correspond to boundary conditions with attractive (repulsive) Casimir forces.
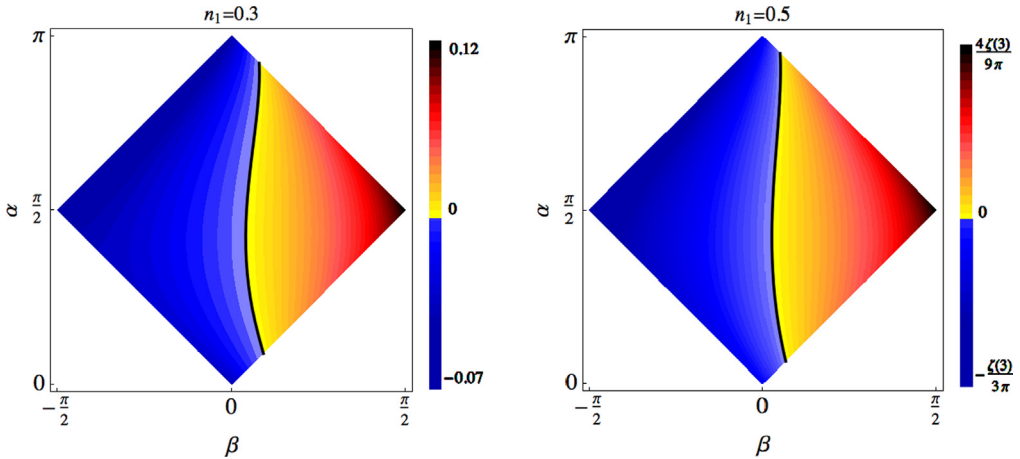

Fig. 9. (Colour online.) Variation of the $c^{(2)}$ coefficient of the Casimir energy in the consistency domain of boundary conditions $|\beta| < \alpha < \pi - |\beta|$ for $n_1 = 0.3$ and $n_1 = \pm 0.5$. Black curves correspond to boundary conditions with vanishing Casimir energy and blue (red) regions correspond to boundary conditions with attractive (repulsive) Casimir forces.

First, we have shown the existence of new boundary conditions which are fully consistent with fundamental requirements of quantum field theory. Some of these conditions can be experimentally implemented. Second, the spectral approach to the calculation of Casimir energy has been revealed as a very useful tool, not only in cases where it can be analytically implemented but also for achieving a very efficient numerical calculation in any case. In this way we analysed the global properties of Casimir energy $E_c(U)$ as a function in the space of all consistent boundary conditions $\mathcal{M}_F$.

We have univocally characterised which boundary conditions induce an attractive Casimir force and which ones a repulsive Casimir force. However, we have been unable to find the underlying physical arguments that characterise the boundary conditions that induce attrac-
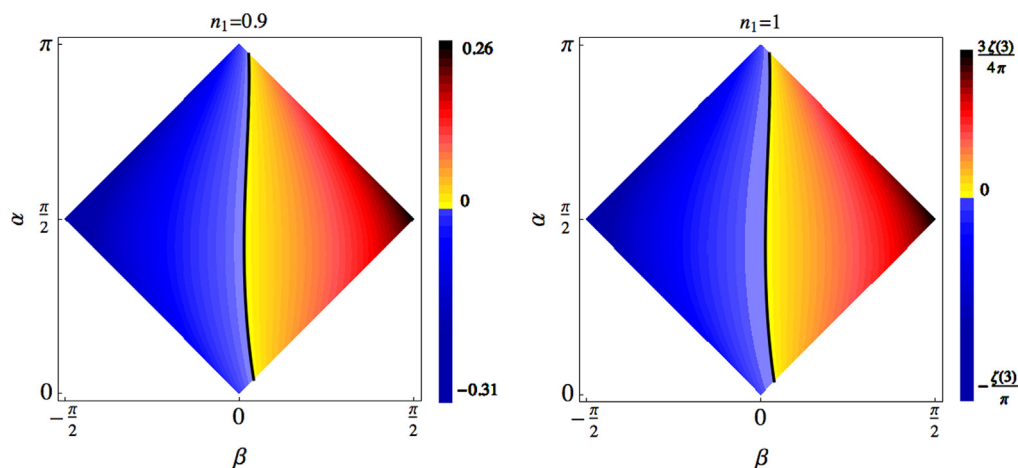
Fig. 10. (Colour online.) Variation of the $c^{(2)}$ coefficient of the Casimir energy in the consistency domain of boundary conditions $|\beta| < \alpha < \pi - |\beta|$ for $n_1 = 0.9$ and $n_1 = 1$. Black curves correspond to boundary conditions with vanishing Casimir energy and blue (red) regions to boundary conditions with attractive (repulsive) Casimir forces.
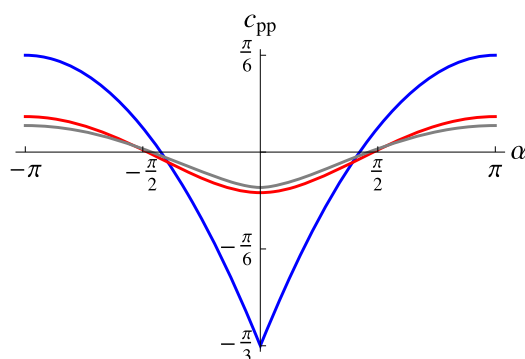

Fig. 11. (Colour online.) Variation of the $c_{pp}^{(D)}$ coefficient of the Casimir energy as a function of $\alpha \in [-\pi, \pi]$ for pseudo-periodic boundary conditions in $D = 1$ (blue), $D = 2$ (gray), $D = 3$ (red). The (weak) first order transition associated to the cusp singularity only appears in one-dimensional systems.

tive or repulsive the Casimir forces, although the algorithm used in the paper provides the simplest mechanism to determine its character. In particular, we have fully characterised the 3-dimensional family of boundary conditions that are in the interface between the attractive and repulsive regimes. This family of Casimirless boundary conditions has a very special property: that their Casimir force vanishes, which may have some interest for physical applications.

We have confirmed that all boundary conditions corresponding to identical bodies are always attractive in agreement with the Kenneth–Klich theorem. In fact, we have shown that the same behaviour holds for bodies with slightly different boundary conditions. A result that follows from the continuity of the Casimir Energy in the space of boundary conditions. In general the repulsive behaviour requires rather different boundary conditions for the two plates.

It is of note that the cusp singularity of pseudo-periodic boundary conditions in $1 + 1$ dimensions at $\alpha = 0$ has disappeared in $2 + 1$ dimensions (Fig. 11). This means that the (weak) first

order phase transition that occurs in $1+1$ dimensions becomes a weaker higher order phase transition in $2+1$ dimensions, and we do not observe any kind of phase transition in 3-dimensional systems at $\alpha = 0$.

The strong convergence properties of the spectral integral that defines the Casimir energy also implies that the Casimir energy function in $\mathcal{M}_F \subset U(2)$ is an holomorphic function when restricted to the interior of the domain. However some singular points can appear at the border of such a space (see Fig. 11), because beyond that border consistency of field theory fails. This property has some physical consequences because if $E_c(\alpha, \beta, \mathbf{n})$ is holomorphic inside $\mathcal{M}_F \cap U(2)$ its extremal values have to be attained at the boundary according to the minimum–maximum principle. This explains why we found the extremal points on the corner of the rhombus.

The extremal points correspond in $1+1$, $2+1$ and $3+1$ dimensions to periodic (minimum) and anti-periodic (maximum) boundary conditions. This property appears to hold in higher dimensions which motivates an interesting conjecture. Periodic boundary conditions always generate the strongest attractive Casimir force between the plates whilst anti-periodic conditions generate the strongest repulsive force. In fact, the conjecture can be proven using inequalities similar to Eq. (4.7).

On the other hand, there is an interesting mismatch between the gradient flow generated by the Casimir energy function and the renormalisation group flow given by [55]

$$\Lambda U_\Lambda^\dagger \partial_\Lambda U_\Lambda = \frac{1}{2}\left(U_\Lambda^\dagger - U_\Lambda\right) \tag{6.1}$$

the fixed points of the RG flow correspond to conformally invariant boundary conditions. However due to the Casimir effect these points are not completely stable. The existence of this property for periodic and anti-periodic boundary conditions is well known from the analysis of the conformal anomaly in $1+1$ dimensions boosted by string theory. Only a small family of boundary conditions (3.21) are conformally invariant and without Casimir force [27]. They can be identified as the boundary conditions sitting at the left and right corners of the rhombus satisfying Eq. (3.22). The field theories with these boundary conditions are conformally invariant and anomaly free, i.e. the vacuum energy vanishes. This opens a new approach to the study of string theory in non-critical dimensions which deserves further study. The stability under these boundary conditions of interacting field theories is also an interesting open question.

Finally, it will be very interesting to generalise the previous analysis to gauge field theories and obtain the dependence of the vacuum energy of gauge field theories on the most general type of boundary conditions from a global perspective.

Acknowledgements

References

[1] H.B.G. Casimir, Proc. K. Ned. Akad. Wet. 51 (1948) 793.

[2] K. Symanzik, Nucl. Phys. B 190 (1981) 1.
[3] A.A. Grib, S.G. Mamaev, V.M. Mostepanenko, Vacuum Quantum Effects in Strong Fields, Friedman Lab. Publishing, St. Petersburg, 1994.
[4] P. Miloni, The Quantum Vacuum: An Introduction to Quantum Electrodynamics, Academic Press, San Diego, 1994.
[5] A. LeClair, G. Mussardo, H. Saleur, S. Skorik, Nucl. Phys. B 453 (1995) 581.
[6] V.M. Mostepanenko, N.N. Trunov, The Casimir Effect and Its Applications, Clarendon Press, Oxford, 1997.
[7] M. Bordag, U. Mohideen, V.M. Mostepanenko, Phys. Rep. 353 (2001) 1.
[8] K.A. Milton, The Casimir Effect: Physical Manifestations of Zero-Point Energy, World Scientific, Singapore, 2001.
[9] N. Graham, R.L. Jaffe, V. Khemani, M. Quandt, M. Scandurra, H. Weigel, Nucl. Phys. B 645 (2002) 49.
[10] N. Graham, et al., Nucl. Phys. B 677 (2004) 379.
[11] A. Scardicchio, R.L. Jaffe, Nucl. Phys. B 704 (2005) 552.
[12] G.L. Klimchitskaya, U. Mohideen, V.M. Mostepanenko, Rev. Mod. Phys. 81 (2009) 1827.
[13] M. Bordag, G.L. Klimchitskaya, U. Mohideen, V.M. Mostepanenko, Advances in the Casimir Effect, Oxford Univ. Press, 2009.
[14] O. Kenneth, I. Klich, Phys. Rev. Lett. 97 (2006) 160401.
[15] C.D. Hoyle, et al., Phys. Rev. Lett. 86 (2001) 1418.
[16] E.G. Adelberger, B.R. Heckel, A.E. Nelson, Annu. Rev. Nucl. Part. Sci. 53 (2003) 77.
[17] D.J. Kapner, et al., Phys. Rev. Lett. 98 (2007) 021101.
[18] R. Onofrio, New J. Phys. 8 (2006) 237.
[19] R.S. Decca, et al., Eur. Phys. J. C 51 (2007) 963.
[20] G.L. Klimchitskaya, U. Mohideen, V.M. Mostepanenko, Phys. Rev. D 86 (2012) 065025.
[21] J.N. Munday, F. Capasso, V.A. Parsegian, Nature 457 (2009) 170.
[22] M. Levin, et al., Phys. Rev. Lett. 105 (2010) 090403.
[23] M. Asorey, G. Marmo, J.M. Muñoz-Castañeda, in: Odintsov, et al. (Eds.), The Casimir Effect and Cosmology, Tomsk State Ped. Univ. Press, 2009, p. 153.
[24] J.M. Muñoz-Castañeda, PhD thesis, Zaragoza University, 2009.
[25] M. Asorey, J.M. Muñoz-Castañeda, Intern. J. Theor. Phys. 50 (2011) 2211.
[26] M. Asorey, J.M. Muñoz-Castañeda, Nanosyst. Phys. Chem. Math. 2 (2012) 20.
[27] M. Asorey, J.M. Muñoz-Castañeda, Int. J. Geom. Meth. Mod. Phys. 9 (2012) 1260017.
[28] M. Asorey, J. Geom. Phys. 11 (1993) 63.
[29] M. Asorey, A. Ibort, G. Marmo, Int. J. Mod. Phys. A 20 (2005) 1001.
[30] A.P. Balachandran, G. Bimonte, G. Marmo, A. Simoni, Nucl. Phys. B 446 (1995) 299.
[31] A.D. Shapere, F. Wilczek, Z. Xiong, Models of topology change, arXiv:1210.3545, 2012.
[32] M. Asorey, et al., Quantum physics and fluctuating topologies: Survey, arXiv:1211.6882 [hep-th], 2012.
[33] M. Asorey, D. García-Álvarez, J.M. Muñoz-Castañeda, J. Phys. A 39 (2006) 6127.
[34] M. Asorey, J.M. Muñoz-Castañeda, J. Phys. A 41 (2008) 164043.
[35] M. Asorey, J.M. Muñoz-Castañeda, J. Phys. A 41 (2008) 304004.
[36] K. Kirsten, Spectral Functions in Mathematics and Physics, Chapman & Hall/CRC, Boca Raton, 2001.
[37] D.V. Vassilevich, Phys. Rep. 388 (2003) 279.
[38] I.G. Avramidi, Nucl. Phys. B 355 (1991) 712;
    I.G. Avramidi, Nucl. Phys. B 509 (1998) 557 (Erratum).
[39] J.M. Muñoz-Castañeda, K. Kirsten, M. Bordag, in preparation.
[40] E. Elizalde, Ten Physical Applications of Spectral Zeta Functions, Lecture Notes in Physics, vol. 35, Springer-Verlag, Berlin, 1995.
[41] S. Blau, M. Visser, A. Wipf, Nucl. Phys. B 310 (1988) 163.
[42] G.N. Watson, Proc. Roy. Soc. London A 95 (1918) 83.
[43] A. Sommerfeld, Partial Differential Equations in Physics, Academic Press, New York, 1949.
[44] N.G. Van Kampen, B.R.A. Nijboer, K. Schram, Phys. Lett. A 26 (1968) 307.
[45] T. Emig, N. Graham, R.L. Jaffe, M. Kardar, Phys. Rev. Lett. 99 (2007) 170403;
    T. Emig, N. Graham, R.L. Jaffe, M. Kardar, Phys. Rev. D 77 (2008) 025005.
[46] A. Lambrecht, P.A. Maia Neto, S. Reynaud, New J. Phys. 8 (2006) 243.
[47] M. Bordag, Phys. Rev. D 73 (2006) 125018.
[48] K.A. Milton, J. Wagner, J. Phys. A 41 (2008) 155402.
[49] M. Abramowitz, I.A. Stegun, Handbook of Mathematical Functions, Dover, New York, 1970.
[50] F.W.J. Olver, et al., NIST Handbook of Mathematical Functions, Cambridge Univ. Press, New York, 2010.
[51] A. Romeo, A.A. Saharian, J. Phys. A 35 (2002) 1297.

[52] C. Farina, Braz. J. Phys. 36 (2006) 1137.
[53] E. Elizalde, A. Romeo, Phys. Rev. D 40 (1989) 436.
[54] J. Ambjørn, S. Wolfram, Ann. Phys. 147 (1983) 1.
[55] M. Asorey, D. García-Álvarez, J.M. Muñoz-Castañeda, J. Phys. A 40 (2007) 6767.